NUMERICAL STUDY OF THE EFFECTS OF MHD AND VISCOUS DISSIPATION ON THE FLOW OF MICROPOLAR NANOFLUID TOWARD A STRETCHING SHEET

[*1]B. Saidulu, [2]MD.Fayaz, [3]B. Raju, [4]M. Sathyanarayana

[*1] Department of Mathematics, Malla Reddy Engineering College for Women, Hyderabad, Telangana, India,500100

[2]Department of Mathematics, University College of Science, Osmania University, Hyderabad, Telangana, India,500007

[3]Department of Computer Science, St. Joseph's Degree & PG College, King Koti, Hyderabad, Telangana, India,5000029

[4]Department of Mathematics & Statistics, St. Joseph's Degree & PG College, King Koti, Hyderabad, Telangana, India,5000029

Email: [1]bandhamssaidulu@gmail.com, [2]fayaz181993@gmail.com , [3]rbownagiri@gmail.com
[4] manthrisathyam926@gmail.com

[*] Corresponding author Email address: bandhamssaidulu@gmail.com

Abstract:

Our study aims to provide a solution to the converted equations for the flow regime. This issue of heat and mass transfer in the magnetohydrodynamic movement of a micropolar via a stretching sheet with the presence of magnetic and viscous dissipation is being investigated in the present work. The existence of micropolar nanofluids distinguishes this flow. For the numerical results, by using MATLAB's inbuilt BVP4C-Technique. The effect of key parameters on the microrotations, including temperature, concentration, and velocities, has been observed. Non-dimensional characteristics, such as Nusselt and Skin friction coefficients but also Sherwood coefficients, are mostly impacted through separate geometric aspects of a flow. According to measurements of the magnetic field, the micropolar component seems to have an adverse effect on all functions except for temperature, while the micro rotational component causes objects to move more slowly but increases the temperature along with concentration distribution. Whenever Prandtl's but also Eckert's numbers rise, the temperature reduces, but as Schmidt's numbers rise, the concentration drops.

Keywords: viscous dissipation, MHD, BVP4C, MATLAB.

Nomenclature			
u, v	$x, y-$Components of velocity	N_b	Brownian motion parameter
b	constant	N_t	Thermophoresis motion parameter
B_0	Magnetitic field	j	microinertia per unit mass (N/kg)
C	concentration of the fluid inside the boundary layer	γ	spin gradient viscosity
C_f	Skin friction coefficient	M	Magnetic parameter
C_p	specific heat at constant pressure $(J/Kg\ K)$	Pr	Prandtl number
C_w	concentration of the fluid at the surface, kg/m^3	Kr	Chemical reaction parameter
C_∞	concentration of the fluid outside the boundary layer, kg/m^3	Sc	Schmidt number
D	Mass diffusion coefficient of the fluid(m^2/s)	K	material parameter
D_B	Brownian diffusion coefficient	κ	vortex viscosity,kg/ms
D_T	Thermophoresis diffusion coefficient	T	Temperature across the thermal boundary layer(k)
E_c	Eckert number	θ	Dimensionless temperature

1.Introduction

During industry sectors, the flow of a viscous incompressible magnetic fluid through a stretching sheet seems to be essential. In particular, it happens when a polymeric layer is produced by a machine or when polymeric strips are drawn. In this study, modification of the picture Plastic melting has been extended and then dried in nanofluid with the principle of electromagnetic induction after becoming injected via a slit plate. Using the electromagnetic induction principle, researchers investigated heat and mass transfer with nanofluid flowing through a stretched layer in magnetohydrodynamic flow. Porous bedrock, sponges including polymerized materials, hydrogels, metals, copolymers, and nano emulsions are just a few instances of the various uses for this issue. Numerous economic growth methods, the fundamental issue with multiple safety zone circulation and heat exchange on a nonlinear stretching sheet that is continuously nonlinear, Over the past several centuries, they have received a lot of interest because of their ability to move in, an otherwise passive liquid flow. Continuous casting provides one illustration, wire drawing, paper production, the production in an otherwise passive liquid flow. the production of plastic illustrations, the deposition of metals and polymers, and metal spinning. Several features of magnetohydrodynamic liquid dynamics have been examined. Rosca and Pop [1] looked into boundary layer instability in the process it travelled across a circular path that might either expand or contract. Bilal et.al [2] showed multiple effusions of synthetical processes along with magnetization impacts using particular flexible-viscous nanofluids. Rout et al. [3] investigated MHD convective flow now with one micropolar liquid bottom in every significant direction about chemical reactions. Heat conduction and micropolar convection were studied by Mishra et al. [4] when the conjunction between a heat source and a transparent stretched layer. Heat transmission in magnetohydrodynamic micropolar circulation over a stretched surface with fluid motion and chemical change by B. saidulu.et.al [5]. electromagnetic effect for uniform convective flow forward into a semi-infinite criterion plate when there are of hall existing strategies by B. Saidulu [6]. Wong and Leon [7] discuss the various industries that use and will use nanofluids in the coming years. Automobiles, devices, biomaterials, and heat transfer mobile apps are among the implementations. Furthermore, researchers from a previous study [8] by Saidur et al. discussed several potential applications for nanofluids throughout their discussion as well. According to many academic studies, every corporate, economic, domestic, and automotive employer is in every industry. Bhattacharyya [9] investigated dynamic heat transfer with stable flow separation and circulation through a moving fluid that was increasingly flowing. Mandal and Mukhopadhyay [10] investigated thermal performance for liquid dynamics over an exponentially increasing porosity membrane using thermal simulation. Olanrewaju et al. [11] moreover, every influence of melted overall heat transmission among the dissolving object circumambient fluid was explored experimentally using the flow separation concept. This has been done therefore in order to better understand this dissolving. Several studies have looked into every influence for dissolving factors and documented their findings over the last several decades [12-14]. Senapati, N., & Dhal, R. K [15] conducted the most recent study on this topic, investigating every influence of slip effects on unstable MHD cyclic circulation in a tube loaded with saturated media thus direction of a crosswise magnetic field and convective steam, as well as mass transfer. Ziya Uddin and Manoj [16] investigated the effect of radiation on magnetohydrodynamic thermal and mass transfer movement on a rising angled porosity warmed plate when there was a natural process., Pramod Kumar et al. [17] reviewed induced magnetic field in the free convective Radiating Stream above Permeable Laminate. Krishna et al. [18] focused entirely on the magnetohydrodynamic rotational circulation of a small creature's capillary motion across diffusive media.

This magnetohydrodynamic movement like an electrolyte solution, a liquid, or a gas across porous material across a semi-infinite, vertically stretched surface was explored by the study of Krishna et al. [19]. Recently Eldabe et al. [20] looked at how heat and mass move inside a magnetohydrodynamic stream of micropolar fluid through a sheet that stretches to heat generation, including viscous dissipation. By A. Ishak et al. [21] The research on flow and heat transmission through a stretched surface is significant because of its various practical uses, like in the polymerization sector, where one works with a stretched thermoplastic material. Another example is in the aviation industry, in which an extending metal sheet is used. Mandal et.al [22] examined how thermal radiation and magnetohydrodynamics affected the convective flow of a micropolar nanofluid across an extended surface with nonhomogeneous heat generation. Srinivasa Raju R et al [23] have studied extended surfaces, separation flow, suction/injection, and porous. Magnetohydrodynamics convective flow now an micropolar fluid under every significant effect about synthetically vibes was the subject of research conducted by Rout et al. [24]. MHD flow of micropolar nanofluid was evaluated by Patel et al. [25] across a stretching/shrinking sheet while radiation was taken into consideration. Heat generation and absorbing influence of nanofluid flow across bidirectional stretching and shrinking sheets were investigated by Zainal [26]. Jayaraj et al. [27] investigated dynamic thermophoretic movement about an adding specific during continuous motion containing viscous fluids across a cool horizontal surface using convective heat transfer having changing characteristics. Raptis [28] investigated the influence of radioactivity upon that movement about a micropolar through a fast-changing surface, including the discovery of raising a radiated variable that decreases heat. Mansour et al. [29] investigated mixed convective heat transfer during magnetohydrodynamics containing a micropolar fluid bounding movement across a spherical concave side using nonhomogeneous mass along with temperature fluxes in a micropolar fluid. The impacts of a rigid wall with gravitational pressures affecting heat along with circulation transmission across diffusive media were studied by Vafai and Tien [30]. Moreover, The subject of unstable magnetohydrodynamic heat conduction containing a hydromagnetic liquid over dual similar porosity surfaces was studied by Zueco et al. [31]. Sami Bataineh et al. [32] investigated the topic of highly formed mixed convective and thermal convection as well as energy transmission inside a microchannel for a micropolar. Magyari [33] investigated the continuous variable viscosity demarcation movements across a curved wall near a Newtonian permeable material to get fresh observations further within the advection problem. Lai and Kulacki [34] investigated the influence that changing viscosity had on combined convection down a stretched surface immersed inside a soaked shrinking media, with powder being dissolved varying like an inverse variation in heat. Very recently, Kalpana et al. [35] described the statistically studied overall influence of thermal convection as the generation of energy from scattered nanoparticles across a curved surface. Panigrahi et al. [36] investigated the influence of an electromagnetic field generated with turbulent kinetic energy containing one-dimensionally polarised fluids via a concentric annular structure. Chen [37] studied the mixed effect that viscoelastic dispersion has on magnetohydrodynamics across a stretched surface in the presence of ambient heat conduction. Recently, Maleki et al. [38] investigated the thermal transport, including flow properties containing quasi-nanoparticles, over a porous stretched sheet with drag force. Adegbie et al. [39] investigated the movement of micropolar on a 2D boundary surface towards this static pressure across a vertical continuously expanding sheet. Patel and Singh [40] exhibit non-equilibrium motion but also heat conduction behaviours during radiation circulation for hydromagnetic nanofluid under the Coriolis effect.

These studies seek to identify a way to solve the problem of heat and mass transfer in a magnetohydrodynamic movement of a micropolar nanofluid through a stretching surface in the case of a magnetic field with viscous dissipation. The equations describing the altered flow regime appear to be nonlinear and can't be obtained computationally. For a numerical explanation of the issue, we used the built-in solution in MATLAB. Investigated would be the effects of various important flow characteristics on the flow profile functions. The results are shown in table and graphic modes.

2.MATHEMATICAL ANALYSIS

Suppose a two-dimensional incompressible, electrically conducting fluid has a sliding plate that generates continuous laminar micropolar fluid flow while maintaining rest. In order to ensure that the y-axis is evaluated perpendicular to the x-axis and the x-axis is calculated forward, the width of a sheet must be determined, through adding up the velocities along the directions x and y, Now let us identify the coordinates properly. Surface-level issues result from an original, microscopic slit. On the sheet, the consecutive hypotheses were investigated under the concept that the view's velocity and length from the slit are inversely proportional. Since it is assumed that the magnetic Reynolds number is low, this produced magnetic field is ignored; Hall influence is disregarded, so there's no imposed electric field; and suppose the fluid's properties are constant and it is also isotropic.

Fig. 1 depicts the issue's flow governing equations for the flow of micropolar fluids covered by the assumption of a boundary

Industrial Engineering Journal
ISSN: 0970-2555
Volume : 53, Issue 3, March : 2024

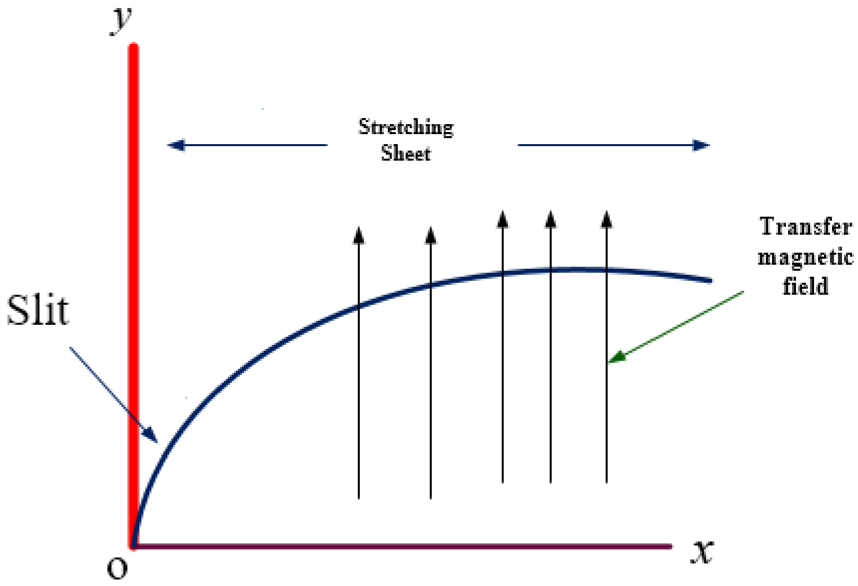

Fig 1: Flow geometry

the equation for continuity:

$$\frac{\partial u}{\partial x}+\frac{\partial v}{\partial y}=0 \tag{1}$$

the equation for momentum

$$u\frac{\partial u}{\partial x}+v\frac{\partial u}{\partial y}=\left(v_f+\frac{k_f}{\rho_f}\right)\frac{\partial^2 u}{\partial^2 y}+\frac{k_f}{\rho_f}\frac{\partial N}{\partial y}-\frac{\sigma B_0{}^2}{\rho_f}u \tag{2}$$

Algebraic expression of angular momentum's:

$$u\frac{\partial N}{\partial x}+v\frac{\partial N}{\partial y}=\frac{\gamma}{j\rho}\frac{\partial^2 N}{\partial y^2}-\frac{k}{j\rho}\left(2N+\frac{\partial N}{\partial y}\right) \tag{3}$$

Algebraic expression of angular momentum's

$$u\frac{\partial T}{\partial x}+v\frac{\partial T}{\partial y}=\frac{k_f}{(\rho C_p)_f}\frac{\partial^2 T}{\partial y^2}+\frac{(\mu_f+k_f)}{(\rho C_p)_f}\left(\frac{\partial u}{\partial y}\right)^2+\frac{\sigma B_0{}^2}{(\rho C_p)_f}u^2 + \frac{(\rho C_p)_p}{(\rho C_p)_f}\left[D_{\mathbf{B}}\frac{\partial C}{\partial y}\frac{\partial T}{\partial y}+\frac{D_T}{T_\infty}\left(\frac{\partial T}{\partial y}\right)^2\right] \tag{4}$$

The equation for concentration:

$$u\frac{\partial C}{\partial x}+v\frac{\partial C}{\partial y}=D_B\frac{\partial^2 C}{\partial y^2}+\frac{D_L}{T_\infty}\frac{\partial^2 T}{\partial y^2} \tag{5}$$

Physical circumstances just

$$\left.\begin{array}{l} u = u_w = bx, v = 0, N = -s\frac{\partial u}{\partial y}, T = T_w, C = C_w \; at \; y = 0 \\ u = 0, N = O, T = T_\infty, C = C_\infty \;\; as \; y \to \infty \end{array}\right\} \quad (6)$$

where its effects of thermophoresis along with Brownian motion have been illustrated mostly by second components in Eq. (4) on the right side. Eq. (3) γ is presumably provided by

$$\gamma = \left(\mu_f + {k_f}/{2}\right) i \quad (7)$$

Furthermore, Assume $i = m/b$ as a standard measurement. While nanoscale influences are negligible but microrotation is reduced to the angular velocity in the limiting situation, The connection (4) is what allows the information provided by equations (1) through (3) to be predicted in the correct presence. Using similarity transformation described below:

$$\eta = \left(\sqrt{\frac{b}{v_f}}\right) y, \; u = bxf'(\eta), v = -\sqrt{bv} f(\eta)$$
$$N = \sqrt{\frac{b^3}{v_f}} x g(\eta), \; \theta(\eta) = \frac{T - T_\infty}{T_w - T_\infty}, T = T_\infty + Ax\theta(x), \quad (8)$$
$$\phi(\eta) = \frac{C - C_\infty}{C_w - C_\infty}, C = C_\infty + Bx\phi(x),$$

Following are the boundary conditions and similarity equations that emerge from inserting Eq. (8) into Eqs. (1) to (6):

$$(1 + K)f''' + ff'' - (f')^2 + Kg' - Mf' = 0 \quad (9)$$

$$\left(1 + \frac{K}{2}\right) g'' + fg' - Gf' - K(2g + f'') = 0 \quad (10)$$

$$\theta'' + Prf\theta' + (1 + K)PrEcf'' + PrMEc(f')^2 + PrNb\theta\phi + PrNt\theta^2 = 0 \quad (11)$$

$$\phi'' + scf\phi' + \frac{Nt}{Nb} Kr\theta'' = 0 \quad (12)$$

$$\left.\begin{array}{ll} f(\eta) = 0, f'(\eta) = 1, N(\eta) = 0, \theta(\eta) = 1, \phi(\eta) = 1 & at \;\; \eta = 0 \\ f'(\eta) = 0, N(\eta) = ,0\; \theta(\eta) = 0, \phi(\eta) = 0 & as \;\; \eta \to \infty \end{array}\right\} \quad (13)$$

However, Eq. (9), which combines given circumstances just at boundaries,

$f'(\infty) = 0$, provides an appropriate result when K = 0.

f(o)=o ,f' (0) & $f'(\infty) = 0$

$$f(\eta) = \frac{1}{2}\left(2 - 2e^{\frac{-1\eta z}{2}}\right), \; z = 2\sqrt{1 + M} \quad (14)$$

shear stress is defined by

$$q_w(x) = -k_f \left(\frac{\partial N}{\partial \zeta}\right)_{y=0} = -k_f(T_w - T_\infty)\sqrt{\frac{b}{v}}\, \theta'(0) \quad (15)$$

Through equation (8)

$$\tau_{w=}(\mu + k)bx\sqrt{\frac{b}{v}}f''(0) \qquad (16)$$

$u_w = bx$ the skin friction coefficient

$$C_f = \tau_w / \left(\rho_f u^2{}_w\right) \qquad (17)$$

From Equation (8) substituted in Equations (15) and (16) and get

$$C_f \sqrt{\mathrm{Re}_w} = (1+k)\, f^{''}(0) \qquad (18)$$

$\mathrm{Re}_w = bx^2 / v_f$ This neighbourhood Reynolds index is f. Surfaces pair tension provided through

$$M_w = \left(\gamma_f \frac{\partial T}{\partial y}\right)_{y=0} = \rho_f b u_w \left(1+ k/2\right) |\, g^{'}(0)\,| \qquad (19)$$

Thermal gradient conductivity has been provided as

$$h(x) = \frac{q_w(x)}{(T_w - T_\infty)} \qquad (20)$$

Nusselt prefix represented as

$$Nu = xh(x)/k_f = -\sqrt{-b / v_f x}\, \theta^{'}(0) \qquad (21)$$

$$Nu/\sqrt{\mathrm{Re}_w} = -\theta^{'}(0) \qquad (22)$$

A source of the local mass flux involves

$$Nu = xh(x)/k_f = -\sqrt{-b / v_f x}\, \theta^{'}(0) \qquad (23)$$

the Sherwood number is defined by

$$sh = \frac{j_w x}{D_f (C_w - C_\infty)} = -\sqrt{b/v_f x}\theta^{'}(0) \qquad (24)$$

Or

$$Sh/\sqrt{\mathrm{Re}_w} = -\theta^{'}(0) \qquad (25)$$

3.METHOD OF SOLUTION:

The set of connected ODEs (9) through (11) and the subsidiary boundary conditions (15) are solved by converting them into an initial value problem.

We set

$y_1 = f, y_2 = f', y_3 = f'', y_4 = g, y_5 = g', y_6 = \theta, y_7 = \theta', y_8 = \phi, y_9 = \phi'$ then the form below is used for nonlinear ODEs.

y'_3 =(M*$y_2 - K$ *y_5+$y_2 * y_2 - y_1 * y_3$)*(1/(1+k))

y'_5 =($K * (2 *, y_4 + y_3)$+ $y_2 * y_4 - y_1 * y_5) * (1/(1 + K/2))$;

$y'_7 = -Pr * y_1 * y_9 - (1 + K) * Pr * Ec * y_3 - Pr * Ec * M * y_2 * y_2 - Pr * N_b * y_5 * y_9 - Pr * N_t * y_7 * y_7$;

$y'_9 = sc * y_1 * y_9 + (N_t/N_b)$ *($Pr * y_1 * y_9 + (1 + K) * Pr * Ec * y_3 + Pr * Ec * M * y_2 * y_2 + Pr * N_b * y_5 * y_9 + Pr * N_t * y_7 * y_7$);

Boundary limits are

$$\left.\begin{array}{c} y_1(0) = 0, y_2(0) = 1, y_4(0) = 0, y_6(0) = 1, y_8(0) = 1 \\ y_2(\infty) = 0, y_4(\infty) = ,0\ y_6(\infty) = 0, y_8(\infty) = 0 \end{array}\right\}$$

These resulting mathematical expressions can be integrated using MATLAB's built-in solver approach. All the above steps will be done again and again until the desired level 10^{-6} of accuracy is reached

4.Results and discussion:

Using the built-in MATLAB programme, the estimated functions of velocity, microrotation, temperature, and concentration are represented graphically in Figures 1–14. The Prandtl number Pr is kept uniform in such investigations at the same quantity of 0.71 used in previous studies, while the impact of the magnetic field parameter(M), Brownian motion parameter (N_b),Thermophoresis motion parameter(N_t), the material parameter(K), the Eckert number (E_c) and the Schmidt number (S_c), is investigated. Some important effects of the dimensionless factors analysed in the dimensionless parameters.

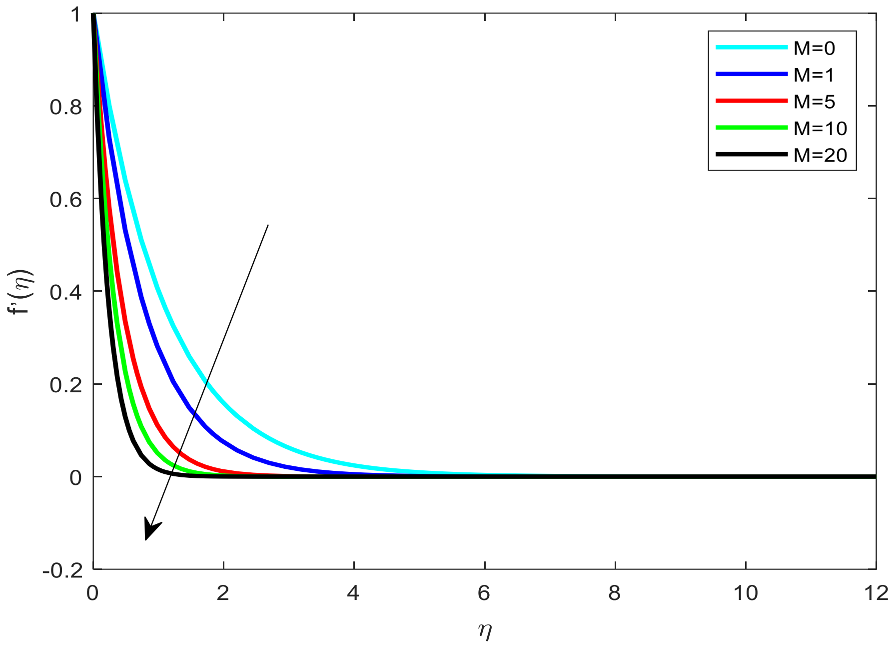

Fig.2: M v/s velocity &Pr=0.71, K=0.2, E_c=0.02, S_c=0.2,N_t=0.1,N_b=0.1.

Figure 2 illustrates how the velocity function depends on the magnetic parameter (M). This demonstrates that velocity decreases as M rises. Which implies that a larger magnetic field might cause a flowing fluid to slow down. But when M increases, the velocity boundary layer's thickness falls. This is because when a magnetic field is introduced to a fluid that conducts electricity, the fluid's velocity slows down.

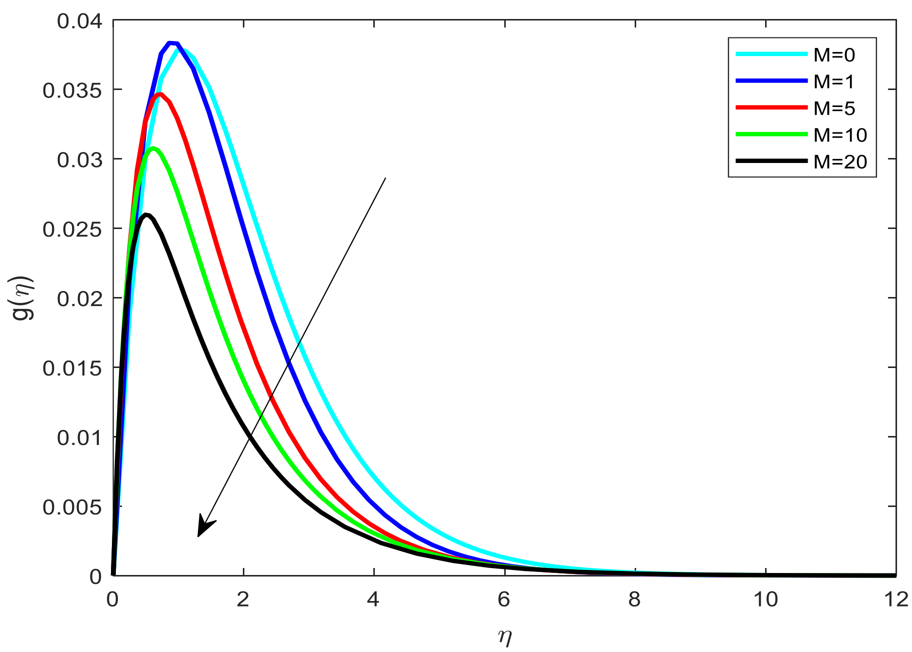

Fig.3: M v/s microrotation & Ec=0.02, Nb= 0.1, K=0.2, Pr=0.71, Nt=0.1,Sc=0.2.

Figure 3 shows how the microrotation distribution changes whenever M changes. Microrotation increases with M increases values.

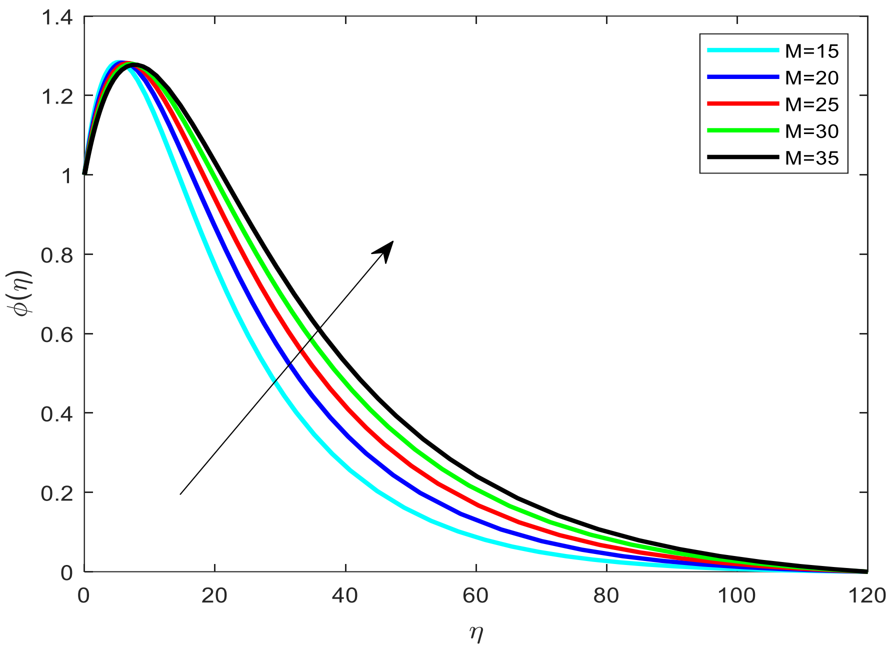

Fig.4: M v/s concentration& & Ec=0.02, Sc=0.2, K=0.2, Nb= 0.1,Pr=0.71, Nt=0.1,

show that magnetic numbers are growing whereas the concentration distribution versus the Figure 4 shows magnetization. Since this is a hypothetical possibility, it is possible that concentration will go up as M goes up, provided such greater Magnetic values inhibits particles transport as a consequence change of address. As a result, the parameter M can be used to control both the temperature and the velocity.

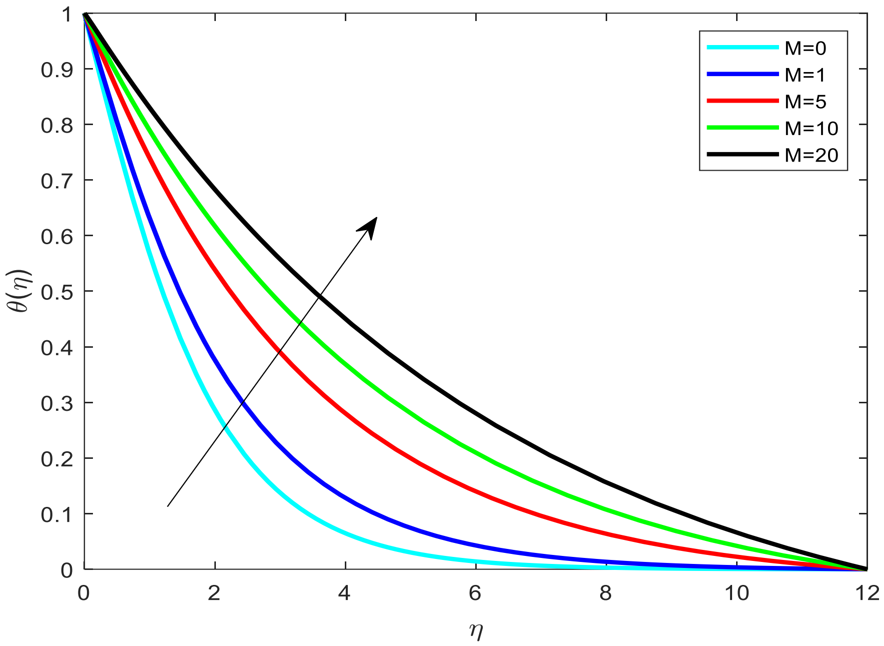

Fig.5: M v/s temperature&, Sc=0.2, Pr=0.71, Ec=0.02, Nb= 0.1,Nt=0.1, K=0.2 .

Figure. 5 depicts visually how temperature and magnetic field strength relate to one another. The graph demonstrates that when M increases, temperature goes up. This temperature is observed to increase till it reaches its highest point at the boundary, then gradually decrease from there. These behaviours can be explained by the Lorentz force, which raises temperature.

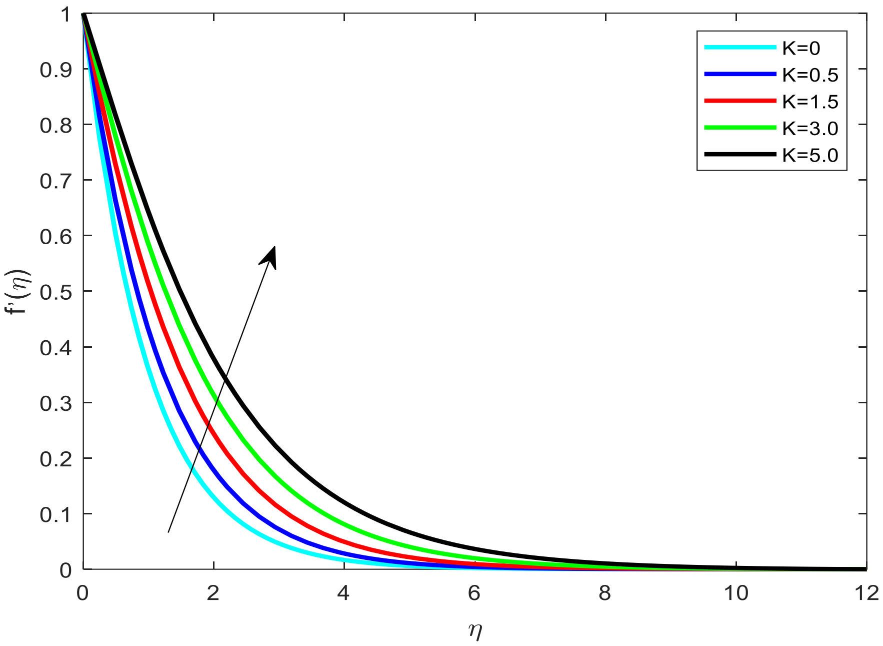

Fig.6: K v/s velocity &Pr=0.71, Ec =0.02, Sc=0.2, Nt =0.1, Nb =0.1, M=0.05.

Figure 6 shows the similarity between velocity and the material parameter K. The graphic unequivocally demonstrates that as K is increased, velocity increases. The material parameter of a drug increases with increasing micro concentration. Consequently, the micro concentration changes the flow field. Such data shows that the material element increases boundary density.

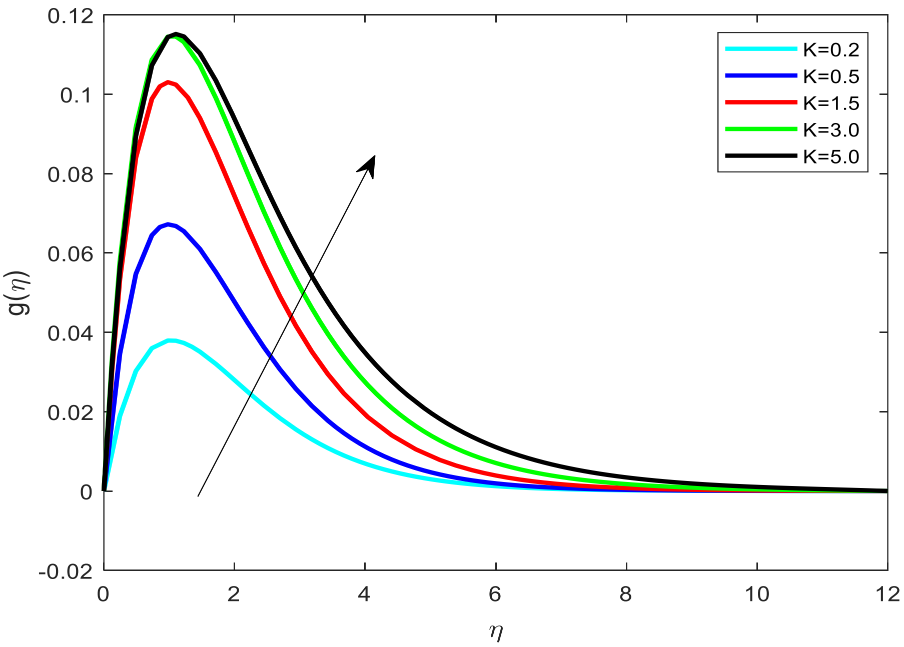

Fig.7: K vs microrotation&Pr=0.71, Ec=0.02, Sc=0.2, Nt =0.1, Nb =0.1, M=0.05

Industrial Engineering Journal
ISSN: 0970-2555
Volume : 53, Issue 3, March : 2024

Figure 7 depicts the influence of a material parameter value upon this microrotation distribution. The microrotation profile was found to rise as material parameter values rises.

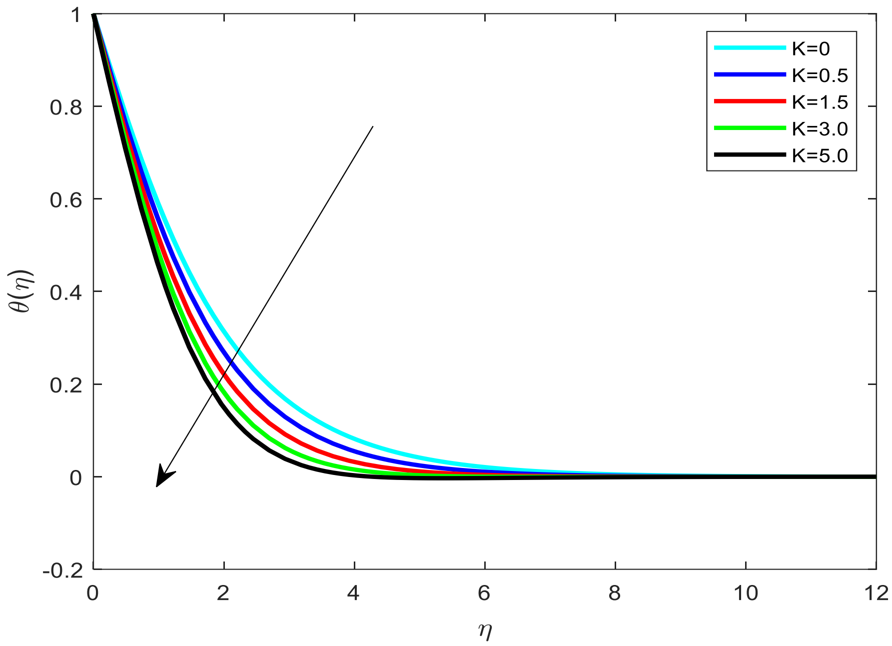

Fig.8: K vs temperature& Pr=0.71, E_c=0.02, S_c=0.2, N_t=0.1, N_b=0.1, M=0.05 &K=0-5.

Fig. 8 depicts schematically how temperature and material characteristics relate to one another. The temperature rises in proportion to the parameter change in a material. The temperature at the border goes up to its highest point before gradually falling.

Industrial Engineering Journal
ISSN: 0970-2555
Volume : 53, Issue 3, March : 2024

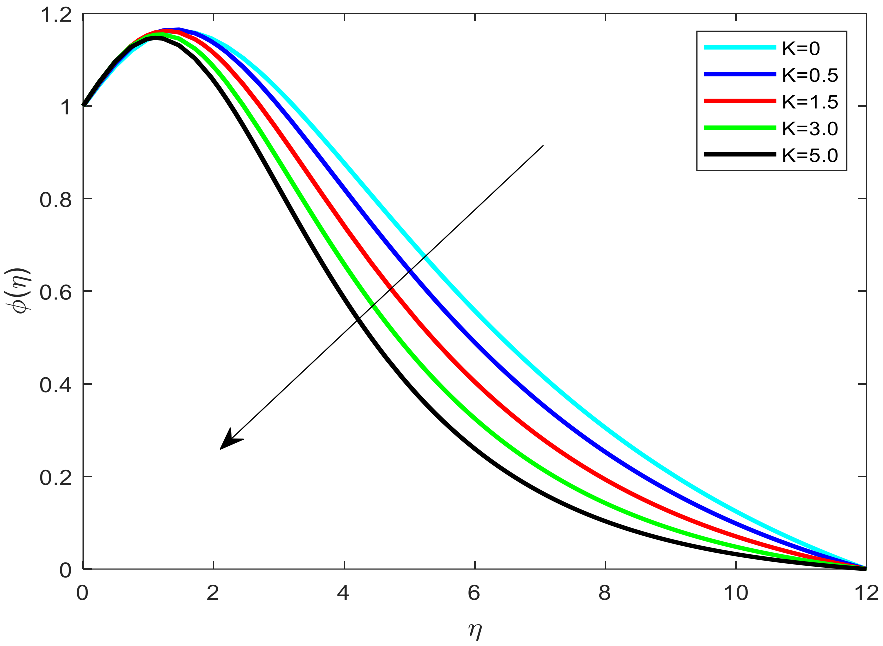

Fig.9: K vs concentration& Pr=0.71, E_c=0.02, S_c=0.2, N_t=0.1, N_b=0.1, M=0.05 &K=0-5.

A profile of the concentration function as a function of the material parameter K is shown in Fig. 9. Results indicate that concentration is steadily deteriorating. The concentration decreases as one increases the material's properties. This variable slightly affects how the concentration function works.

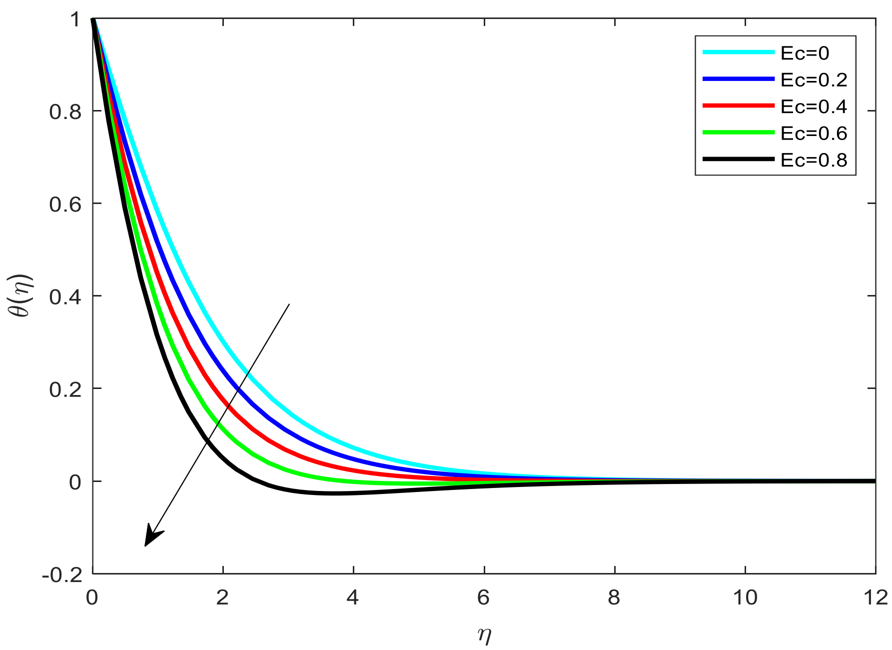

Fig.10: E_c vs temperature& Pr=0.71, Sc=0.2, Nt =0.1, Nb =0.1, M=0.05. K=0.2

Industrial Engineering Journal
ISSN: 0970-2555
Volume : 53, Issue 3, March : 2024

The temperature distribution as a function of the Eckert number Ec is shown in Fig. 10. Temperature and Eckert number are inversely proportional. While the temperature increases to a maximum at the border for low Ec values and then declines slowly from there, it rises to a maximum for high E values. The boundary layer's velocity distribution will be substantial if the Eckert number is large.

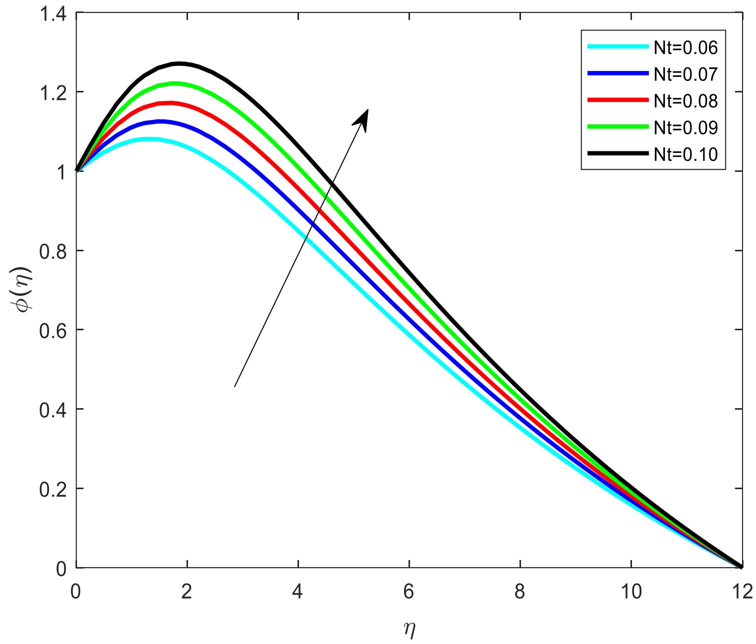

Fig.11: $N_t$vs concentration&Pr=0.71, K=0.2,N_b=0.1, M=0.05,E_c=0.02. & N_t=0.06-0.10.

Illustration 11 was created so the impact could be seen on the concentration distribution. So, when the level of such a thermophoretic characteristic is increased, the presence of a subsequent rise inside that concentration distribution can be seen. Through this, they indicate how an excessive number of nanoparticles move towards warm surfaces, causing a rise in volume fraction variation.

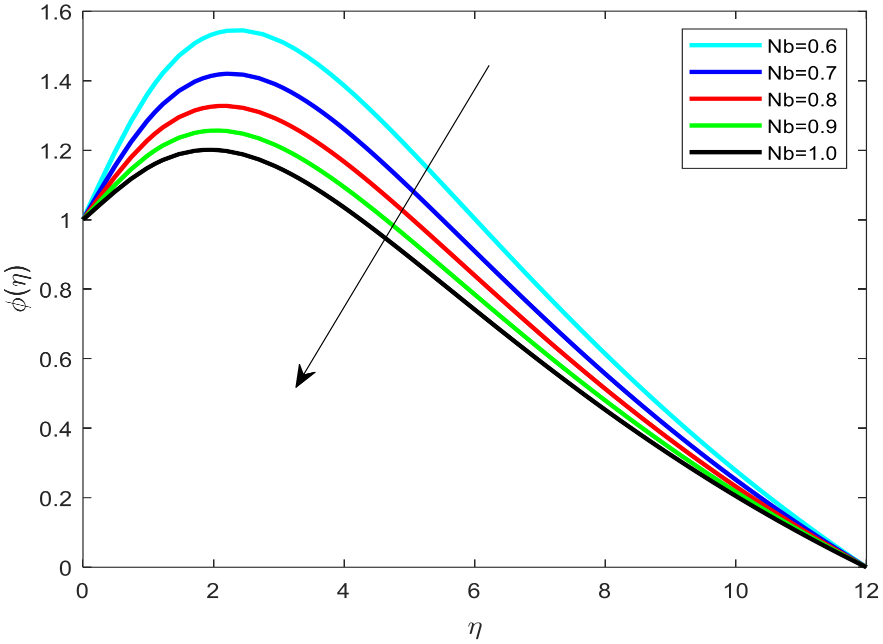

Fig.12: Nb vs concentration&Pr=0.71, K=0.2,N_t=0.1, M=0.05,E_c=0.02.S_c =0.1& N_b=0.6-1.0.

Figure 12 illustrates the effect that a certain Brownian motion factor has on concentration distribution. The graph shows that as the quantity increases, as in a Brownian motion, the concentration distribution becomes less than its initial value. An increase throughout the Brownian motion factor causes a decrease in concentration distribution along with a density-containing boundary layer.

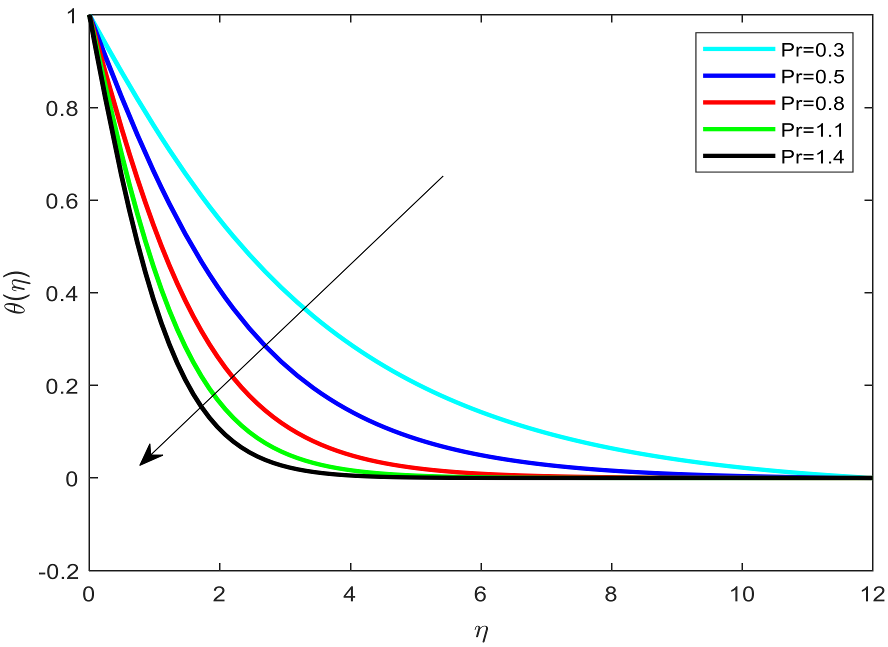

Fig.13: Pr vs temperature &K=0.2, S_c=0.2,N_t=0.1,Nb =0.1, M=0.05,E_c=0.02 & Pr=0.71

Picture 13 depicts the temperature distribution fluctuation that can be attributed to the Prandtl number. It was shown that as the number in regards to Pr increased, there was a corresponding decrease in temperature as well as the density of the boundary layer. It indicates a higher significance in terms of Pr causing a decrease in thermal diffusivity.

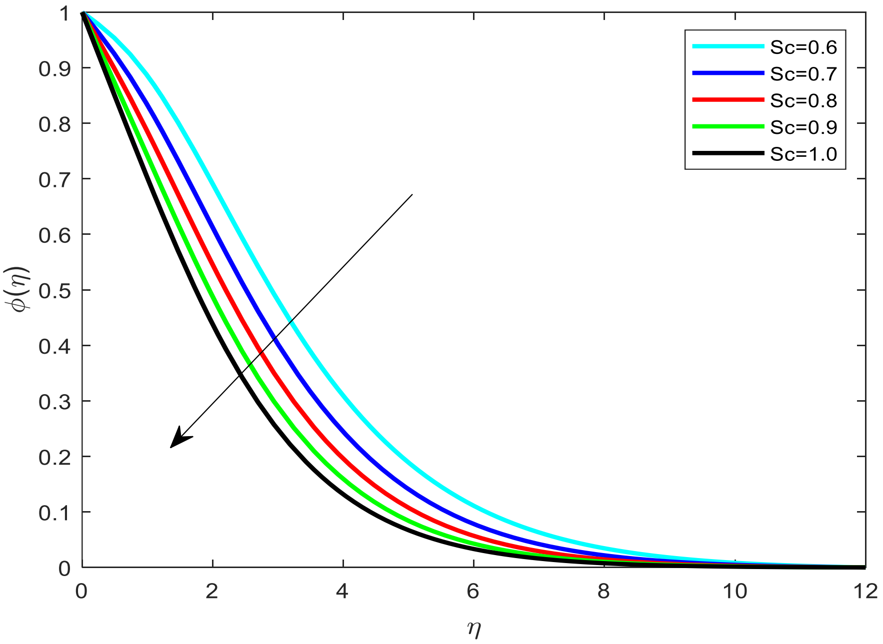

fig 14: Sc vs concentration &K=0.2, N_t=0.1,N_b=0.1, M=0.05,E_c=0.02, Pr=0.71&S_c=0.6-1.0.

It has been demonstrated that this maximum level for Sc, also known as a greater variety along with lower diffusivity, brings about a decrease in its concentration in the complete wound-up flow zone. An increase in the Schmidt value maintains a relationship toward the solute diffusion coefficient that is the lowest feasible; as a result, it is also possible to obtain the most surface distribution of the prevention effect. When the Schmidt-Factor is increased to a higher value, the concentration decreases. As a result, as the Schmidt number increases, the depth of such concentration flow separation decreases. Increasing the Schmidt number implies increasing momentum diffusion versus mass diffusion, which results in a reduction across the concentration distribution. Table 1 presents a comparison of $-f''(0)$ for a variety of different M, K values in the absence of any other factors. Table 2 presents a comparison of $g'(0)$ for a variety of different M, K values in the absence of any other factors. Table 3 presents a comparison of $-\theta'(0)$ for a variety of different M, K values in the absence of any other factors. Table 4 presents a comparison of $-ø'(0)$ for a variety of different M, K values in the absence of any other factors.

Table1: comparison $-f''(0)$ considering a Wide Range like M as well as Quantities k $with\ Ec = s = 0$.

M	K	Eldabe. N.T and Mahmoud E.M. Ouaf [20] Previous results $-f''(0)$	Present results $-f''(0)$
0.0	0.2	0.9098	0.909739
0.5	0.2	1.1148	1.114375
1.0	0.2	1.2871	1.287135
	0.0	1.4142	1.414214
	0.5	1.1407	1.140766
	2.0	0.7696	0.769666

Table2:comparison $g'(0)$ versus M , K values along $Ec = s = 0$.

M	K	Eldabe. N.T and Mahmoud E.M. Ouaf [20] Previous results $g'(0)$	Present results $g'(0)$
0.0	0.2	0.0950	0.094997
0.5	0.2	0.1051	0.105090
1.0	0.2	0.1121	0.112125
	0.0	0	0.000000
	0.5	0.2112	0.211167
	2.0	0.3586	0.358554

Table3: comparison $-\theta'(0)$ versus M, K values along $Ec = s = 0$.

M	K	Eldabe. N.T and Mahmoud E.M. Ouaf [20]. Previous results $-\theta'(0)$	Present results $-\theta'(0)$
0.0	0.2	0.4688	0.476330

Table4: comparison $-\emptyset'(0)$ versus M, K values along $Ec = s = 0$.

M	K	Eldabe. N. T and Mahmoud E.M.Ouaf [20] Previous results $-\emptyset'(0)$	Present results $-\emptyset'(0)$
0.0	0.2	0.2149	0.199278
0.5	0.2	0.1972	0.186692
1.0	0.2	0.1857	0.145325
	0.0	0.1790	0.129530
	0.5	0.1938	0.164173
	2.0	0.2204	0.222371

CONCLUSIONS

We were successful in investigating how different objective factors influence magnetohydrodynamic heat and mass transfer inside a micropolar nanofluid, incompressible passing across a stretching sheet involving ohmic heating and viscous dissipation. By using the MATLAB built-in solver method, the governing differential equations are transformed into a linear form and solved numerically, when the flow fields were subjected to a variety of non-dimensional factors. The conclusions are drawn in consideration of the investigation's results.

- With increasing magnetic parameter M, velocities and Nusselt profiles decrease
- Shear stress, couple stress, temperature, and concentration profiles increase with increasing magnetic parameters.
- Velocities and Nusselt-Profile increase with increasing values of material parameter K.
- The temperature effect increases with increasing Prandtl and Eckert numbers.
- The concentration effect increases with increasing Schmidt- or Brownian-numbers.

- The temperature effect increases with increasing Prandtl and Eckert numbers.

REFERNACE:

1) Rosca, N. C. & Pop, I. Unsteady boundary layer flow over a permeable curved stretching/shrinking surface. *Euro. J. Mech. B/Fluids.* **51**, 61–67 (2015).

2) Ramzan, M. & Bilal, M. provided three-dimensional flow of an elastico-viscous nanofluid a chemical reaction and magnetic field effects. journal of molecular liquids,215,212,220.

3) Rout, P., Sahoo, S., Dash, G., and Mishra, S. Chemical reaction effect on MHD free convection flow in a micropolar fluid. Alexandria Engineering Journal, 55(3), 2016, 2967-2973. https://doi.org/10.1016/j.aej.2016.04.033.

4) Mishra, S., Khan, I., Al-mdallal, Q., and Asifa, T.: Free convective micropolar fluid flow and heat transfer over a shrinking sheet with heat source. Case Studies in Thermal Engineering, 11, 2018, 113-119. https://doi.org/10.1016/j.csite.2018.01.005.

5) Saidulu, B., and Reddy, K. S.: Evaluation of combined heat and mass transfer in hydromagnetic micropolar flow along a stretching sheet when viscous dissipation and chemical reaction is present. Partial Differential Equations in Applied Mathematics, 2023, 7, 100467. https://doi.org/10.1016/j.padiff.2022.100467.

6) Saidulu, B." Role of Magnetic Field on Natural Convective Towards a Semi-Infinite Vertically Inclined Plate in Presence of Hall Current with Numerical Solutions: A Finite Difference Technique ", International Journal of Scientific and Innovative Mathematical Research, vol. 6, no. 2, p. 25-40, 2018., http://dx.doi.org/10.20431/2347-3142.0602003.

7) Wong K.V, and Leon, O.D, "Applications of nanofluids: current and future," Advances in Mechanical Engineering, vol. 2010, Article ID 519659, 11 pages, 2010.

8) Saidur,R, K. Y. Leong, and H. A. Mohammad, "A review on applications and challenges of nanofluids," Renewable and Sustainable Energy Reviews, vol. 15, no. 3, pp. 1646–1668, 2011.

9) Bhattacharyya, K. Steady boundary layer flow and reactive mass transfer past an exponentially stretching surface in an exponentially moving free stream. Journal of the Egyptian Mathematical Society, 20(3), 2012, pp.223-228.

10) Mandal, I. C., and Mukhopadhyay, S.: Heat transfer analysis for fluid flow over an exponentially stretching porous sheet with surface heat flux in porous medium. Ain Shams Engineering Journal, 4(1), 2013, pp.103-110.

11) Olanrewaju PO, Arulogun O .T, Adebimpe K. Internal heat generation effect on thermal boundary layer with a convective surface boundary condition. Am J Fluid Dyn 2012;2:1–4. http://dx.doi.org/10.5923/j.ajfd.20120201.01.

12) Yacob N, Ishak A, Pop I. Melting heat transfer in boundary layer stagnation-point flow towards a stretching/shrinking sheet in a micropolar fluid. Computers and Fluids 2011; 47:16–21. http://dx.doi.org/10.1016/j.compfluid.2011.01.040.

13) Rasekh A, Ganji DD, Tavakoli S, Naeejee S. Melting effect on steady laminar flow of a Micropolar fluid over a stagnation point on a vertical surface. J Eng Phy Thermophys 2013;86: 210–1216.

14) Hayat T, Hussain M, Awais M, Obaidat S. Melting heat transfer in a boundary layer flow of a second grade fluid under Soret and Dufour effects. Int J Numer Methods Heat Fluid Flow 2013;23:1155–68. http://dx.doi.org/10.1108/HFF-09-2011-0182.

15) Senapati, N., & Dhal, R. K (2013). Effect of Slip Condition on Unsteady MHD Oscillatory Flo Gc w in a Channel Filled with Porous Medium with Heat Radiation and Mass Transfer, Int. J. Appl. Math. Statist. Sci., [Online]. 2, pp. 11-20. Available: http.journalajst.com/sites/default/files/1536.pdf.

16) Uddin. Z, Manoj.K, (2010). Radiation Effect on Unsteady MHD Heat and Mass Transfer Flow on a Moving Inclined Porous Heated Plate in the Presence of Chemical Reaction, Int. J. Math. Mod., Simul. Appl. [Online]. 3, pp. 155-163. Available: www.academia.edu.

17) Kumar P, Balasiddulumalga S, Matta L, Appidi. Heat Transfer Reaction on a Viscous Dissipative Free Convective Radiating Stream over a Permeable Laminate within Presence of Induced Magnetic Field. International Journal of Innovative Technology and Exploring Engineering. 2020;8(3):2057–2062. doi:10.35940/ijitee.C8887.019320.

18) Krishna MV, Sravanthi CS, Gorla RSR. Hall and ion slip effects on MHD rotating flow of ciliary propulsion of microscopic organism through porous media. Int Commun Heat MassTransfer2020;112.doi:https://doi.org/10.1016/j. icheatmasstransfer.2020.104500104500.

19) Krishna MV, Jyothi K, Chamkha AJ. Heat and mass transfer on MHD flow of second-grade fluid through porous medium over a semi-infinite vertical stretching sheet. J Porous media 2020;23(8):751–65. doi: https://doi.org/ 10.1615/JPorMedia.2020023817.

20) Eldabe .N.T, and Mahmoud E.M. Ouaf, Chebyshev finite difference method for heat and mass transfer in a hydromagnetic flow of a micropolar fluid past a stretching surface with Ohmic heating and viscous dissipation, Appl. Math. Comput. 177 (2) (2006) 561–571.

21) Ishak.A, Nazar.R and Pop.I, “Unsteady mixed convection boundary layer flow due to a stretching vertical surface,” The Arabian Journal for Science and Engineering B, vol. 31, no. 2, pp. 165–182, 2006.

22) Pal D, Mandal G. Thermal radiation and MHD effects on boundary layer flow of micropolar nanofluid past a stretching sheet with non-uniform heat source/sink. Int J Mech Sci. 2017; 126:308–318.

23) Srinivasa Raju R, Anil Kumar M, Dharmendar Reddy Y. Unsteady MHD free convective flow past a vertical porous plate with variable suction. ARPN J Eng Appl Sci. 2016;11(23):13608–13616.

24) Rout, P., Sahoo, S., Dash, G., and Mishra, S. Chemical reaction effect on MHD free convection flow in a micropolar fluid. Alexandria Engineering Journal, 55(3), 2016, 2967-2973. https://doi.org/10.1016/j.aej.2016.04.033.

25) Patel, H. R., Mittal, A. S., and Darji, R. R.: MHD flow of micropolar nanofluid over a stretching/shrinking sheet considering radiation. International Communications in Heat andMassTransfer,108,2019,104322.https://doi.org/10.1016/j.icheatmasstransfer.2019.104322

26) Zainal, N. A., Nazar, R., Naganthran, K., & Pop, I. (2021). Heat generation/absorption effect on MHD flow of hybrid nanofluid over bidirectional exponential stretching/shrinking sheet. Chinese Journal of Physics, 69, 118-133. https://doi.org/10.1016/j.cjph.2020.12.002.

27) S. Jayaraj, K.K. Dinesh, K.L. Pillai. Heat Mass Transfer, 1999; 34, 469–475.

28) A. Raptis. Int. J. Heat Mass Transfer, 1998; 4, 2865–2866.

29) Mansour MA, El-Hakiem MA, El Kabeir SM. Heat and mass transfer in magnetohydrodynamic flow of micropolar fluid on a circular cylinder with uniform heat and mass flux. Journal of Magnetism and Magnetic Materials 2000; 220:259–270.

30) Vafai K, Tien CL. Boundary and inertia effects on flow and heat transfer in porous media. Int J Heat Mass Transf 1981; 24:195–203.

31) Zueco J, Eguia P, Lopez-Ochoa LM, Collazo J, Patino D. Unsteady MHD free convection of a micro polar fluid between two parallel porous vertical walls with convection from the ambient. Int Comm Heat Mass Transf 2009; 36:203–209.

32) Sami Bataineh A, Noorani MSM, Hashim I. Solution of fully developed free convection of a micropolar fluid in a vertical channel by homotopy analysis method. Int J Numer Methods in Fluids 2009;60:779.

33) Magyari E. A New Insight into the Convective Boundary Condition. Transp Porous Med 2013;99(1):55–71.

34) Lai FC, Kulacki FA. The effect of variable viscosity on convective heat transfer along a vertical surface in a saturated porous medium. Int J Heat Mass Transfer 1990;33(5):1028–1031.

35) Kalpana G, Mathira KR, Iyengar SS. Numerical computation on Marangoni convective flow of two-phase MHD dusty nanofluids under Brownian motion and thermophoresis effects. Heat Transf—Asian Res. 2020; 49:626-650. https://doi.org/10.1002/htj.21630.

36) Panigrahi L, Panda J, Kumar D, Sahoo SS. Analytical investigation of polar fluid flow with induced magnetic field in concentric annular region. Heat Transfer. 2020;49(6):3943-3957. https://doi.org/10.1002/htj.21816.

37) Chen CH. Combined effects of Joule heating and viscous dissipation on magnetohydrodynamic flow past a permeable stretching surface with free convection and radiative heat transfer. J Heat Transf. 2010;132, 064503.

38) Maleki H, Safaei MR, Alrashed AA, Kasaeian A. Flow and heat transfer in non-Newtonian nanofluids over porous surfaces. J Thermal Anal Calorim. 2019; 135:1655–66.

39) Adegbie, S.K.; Kọrikọ, O.K.; Animasaun, I.L. Melting heat transfer effects on stagnation point flow of micropolar fluid with variable dynamic viscosity and thermal conductivity at constant vortex viscosity. J. Niger. Math. Soc. 2016, 35, 34–47.

40) Patel, H.R.; Singh, R. Thermophoresis, Brownian motion and non-linear thermal radiation effects on mixed convection MHD micropolar fluid flow due to nonlinear stretched sheet in porous medium with viscous dissipation, joule heating and convective boundary condition. Int. Commun. Heat Mass Transf. 2019, 107, 68–92.